Supplementary Information

Growth landscape formed by perception and import of glucose in yeast

Hyun Youk & Alexander van Oudenaarden

DISCUSSION OF OUR GROWTH MODEL

When the cell's glucose uptake rate r is lower than r_c, an increase in the extracellular glucose concentration causes two counteracting effects (Fig. 3b). First, since the Hxt is a passive transporter, it leads to an increased glucose uptake rate (which tends to increase the growth rate). Second, it causes the cell to perceive a higher amount of glucose (which tends to decrease the growth rate). This counteracting interaction between the two mechanisms – glucose perception and uptake – determines how the growth rate changes (i.e., whether it increases or decreases) as a result of an increase in the extracellular glucose level. The effect of this interaction on the growth rate is quantified by $P(g)\ln\left(\frac{r}{r_c}\right)$ which couples the two mechanisms. In particular, if g_0 and r_0 are glucose concentration and uptake rate of a cell in growth environment 'A', while g_1 and r_1 are for growth environment 'B', then the cell grows faster in environment 'B' than in environment 'A' if the following inequality is satisfied:

$$P(g_0)\ln\left(\frac{r_0}{r_c}\right) < P(g_1)\ln\left(\frac{r_1}{r_c}\right) \qquad \textbf{[1]}$$

Due to the counteracting nature of the two mechanisms, a higher uptake rate ($r_0 < r_1$) and a higher glucose level ($g_0 < g_1$) do not guarantee that above inequality will hold. This can be visualized in the growth landscape (Fig. 3c).

Balancing glucose perception and import.

While an increase in the amount of glucose in the cell's surrounding causes the Hxt to transport glucose faster due to the passive nature of the Hxt, it also results in the cell perceiving a higher amount of glucose that can decrease the cell's growth rate as seen Figs. 3b-c (unless the cell's uptake rate is larger than r_c). If the cell wishes to prevent its growth rate from decreasing in this situation, it has to not only increase its uptake rate but do so by at least a certain minimum amount. The cell can achieve this by changing both the number and type of Hxt it makes as a function of glucose. To formalize this

notion, let $N_{HXTn}(g)$ be the number of Hxt type "*n*" the cell makes when it senses a particular concentration of glucose *g* in its surrounding. Then the cell's total uptake rate *r* is a function $r = r(\{N_{HXTn}(g)\}, g)$ where $\{N_{HXTn}(g)\}$ is the set of all types of Hxts made by the cell. The growth rate $\mu(\{N_{HXTn}(g)\}, g))$ then is a curve parameterized by *g*: it is a particular "growth trajectory" in the space of all possible growth rates (Fig. 3c). Hence the particular set $\{N_{HXTn}(g)\}$, hard-wired into the cell by transcriptional regulation of the *HXT* genes, determines the particular "growth trajectory". Using the expression for growth rate $\mu(r,g) = P(g)\ln\left(\frac{r}{r_c}\right) + \mu_c$ obtained in Fig. 3b, the requirement that the cell's growth rate never decreases whenever *g* increases ($d\mu/dg \geq 0$) means that the following inequality has to be satisfied at all points on its growth trajectory:

$$\text{(Perception)} \quad \frac{dP/dg}{P} \leq \frac{d\ln(r/r_c)/dg}{\ln(r_c/r)} \quad \text{(Import).} \qquad \textbf{[2]}$$

Those parts of the growth trajectory where above inequality is not met correspond to the cell's growth rate decreasing despite an increase in *g*. Notice the left hand side of Eqn.[2] involves only the effect of glucose perception while the right hand side involves only the glucose import. Above inequality represents the balance of fractional changes due to these two separate effects. Any synthetic rewiring of the transcriptional regulation of the *HXT* genes, leading to changing the set $\{N_{HXTi}(g)\}$ from the wild-type values, should be done mindful of above inequality: a lesson learned from the "single-*HXT*" strains.

Possible molecular mechanisms underlying the effects of glucose perception and import.

Glucose metabolism, involving thousands of chemical reactions and numerous intracellular events (gene regulations, post-transcriptional modifications, etc.), is a complex process. But the equation for growth rate $\mu(r,g) = P(g)\ln\left(\frac{r}{r_c}\right) + \mu_c$ obtained in Fig. 3b shows us that such a complex set of components can work in concert to yield a simple description. Since glucose metabolism involves thousands of intracellular activities ranging from metabolic reactions, transcription of many genes, and post-transcriptional modifications, it is difficult to pinpoint to a single, or most likely, many

correlated molecular events that underlie the phenomenological growth model revealed in our study. As a case example, a recent microarray study[1] has shown that hundreds of genes involved in ribosomal biogenesis, which are energetically very costly due to their relatively short half-lives, are up-regulated by many decade-folds as the extracellular glucose concentration is increased from 0.01%, to 0.1%, and then to1% w/vol. Future studies that look at the global expression levels while varying the glucose perception and import independently of each other may help in distinguishing what fraction of these expression level changes are due to (1) changes in the perception of extracellular glucose level as opposed to (2) changes in the glucose import rate. Such a study would shine light into the transcriptional regulations that may be responsible for the growth effects embodied in our growth model. In addition, a large-scale study that measures the changes in the metabolites (using mass spectrometry, for instance) while the cell's perception and import of glucose are varied independently of each other over a wide range will further elucidate what is likely to be a vast number of molecular mechanisms underlying the phenomenological growth model uncovered in our study. It is well known that glucose-mediated post-transcriptional modifications exist, especially of metabolic proteins[2]. Measuring how these events are affected separately by glucose perception and import on a global scale would be difficult but worthwhile. Decupling the glucose perception from glucose import in large-scale studies will yield valuable insights in understanding the vast molecular events that are likely working in concert to produce the phenomenological growth model revealed in our study.

SUPPLEMENTARY FIGURES

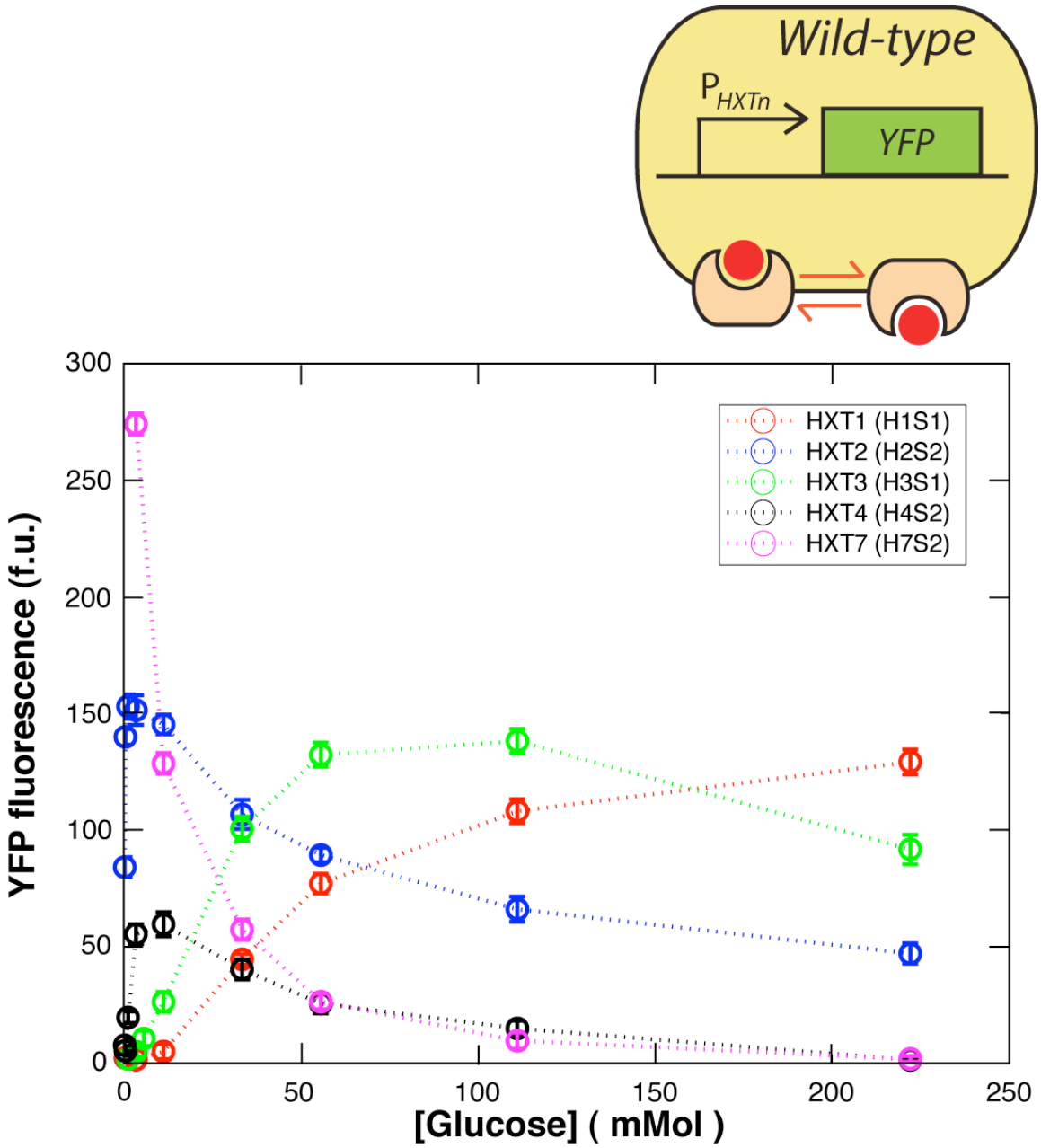

Supplementary Figure 1: Expression levels of *HXT* genes in wild-type strain (CEN.PK2-1C) measured using YFP reporters (used "Wild-type P_{HXTn}:YFP" strains; see "strain list"). As the extracellular glucose concentration varies, the expression level of each *HXT* gene in the wild-type strain changes. Two of the glucose sensors, Snf3 and Rgt2, initiate the signal transduction that results in these expression patterns. This result was originally reported in a previous work[3]. We have reproduced it here for the sake of completeness. Error bars, s.e.m.; *n*=3.

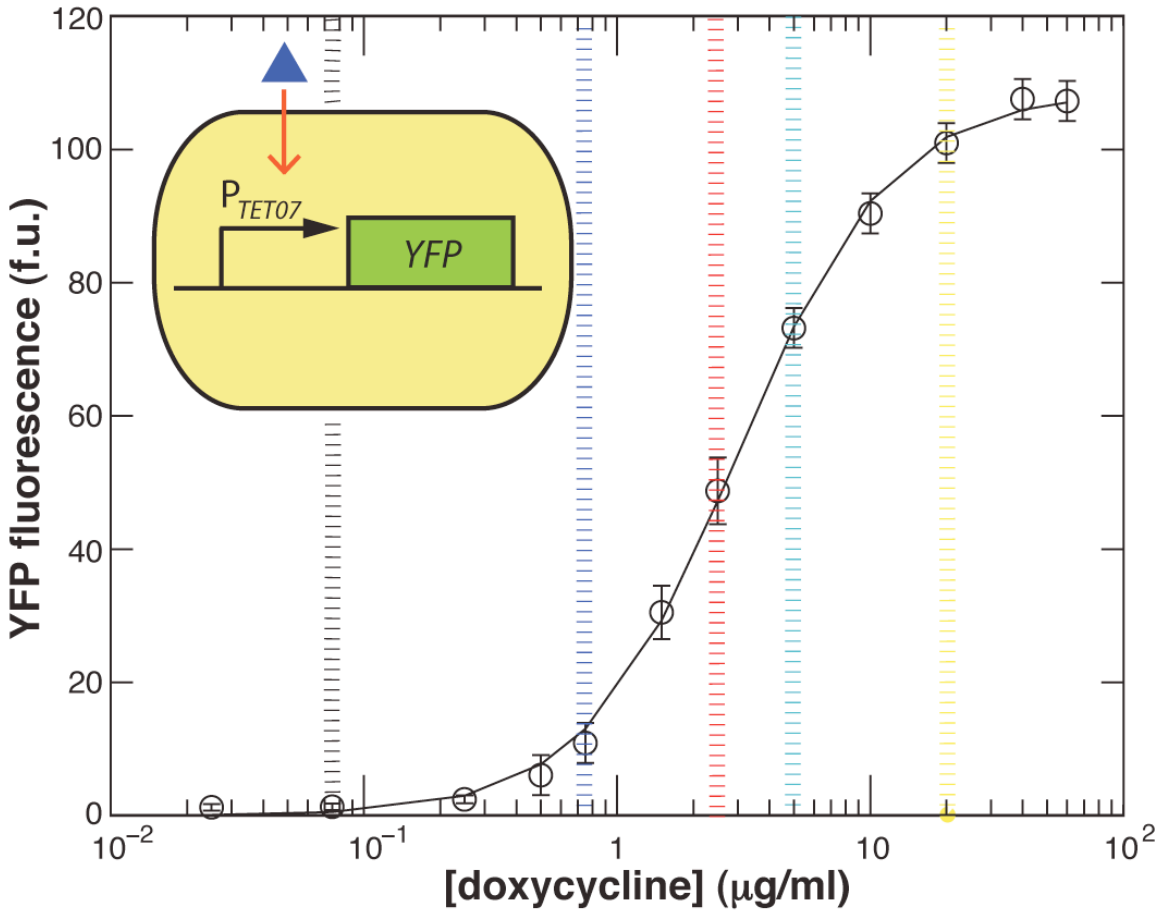

Supplementary Figure 2: Inducibility of P_{TET07} inferred from YFP fluorescence as a function of doxycycline concentration in the HY4DCal5 strain. HY4DCal5 and the single-*HXT* strains were all constructed using the same background strain HY4D1. Hence we can infer the inducibility of the promoter P_{TET07} in the single-*HXT* strains from this induction curve measured in the HY4DCal5 strain. The fluorescence data shown here were obtained while the cells were in log-phase growth in a standard synthetic media with 2% maltose and the indicated doxycycline concentration. The colored vertical dashed lines indicate the concentrations of doxycyline used in subsequent supplementary figures for characterizing the single-*HXT* strains. Error bars, s.e.m.; *n*=3.

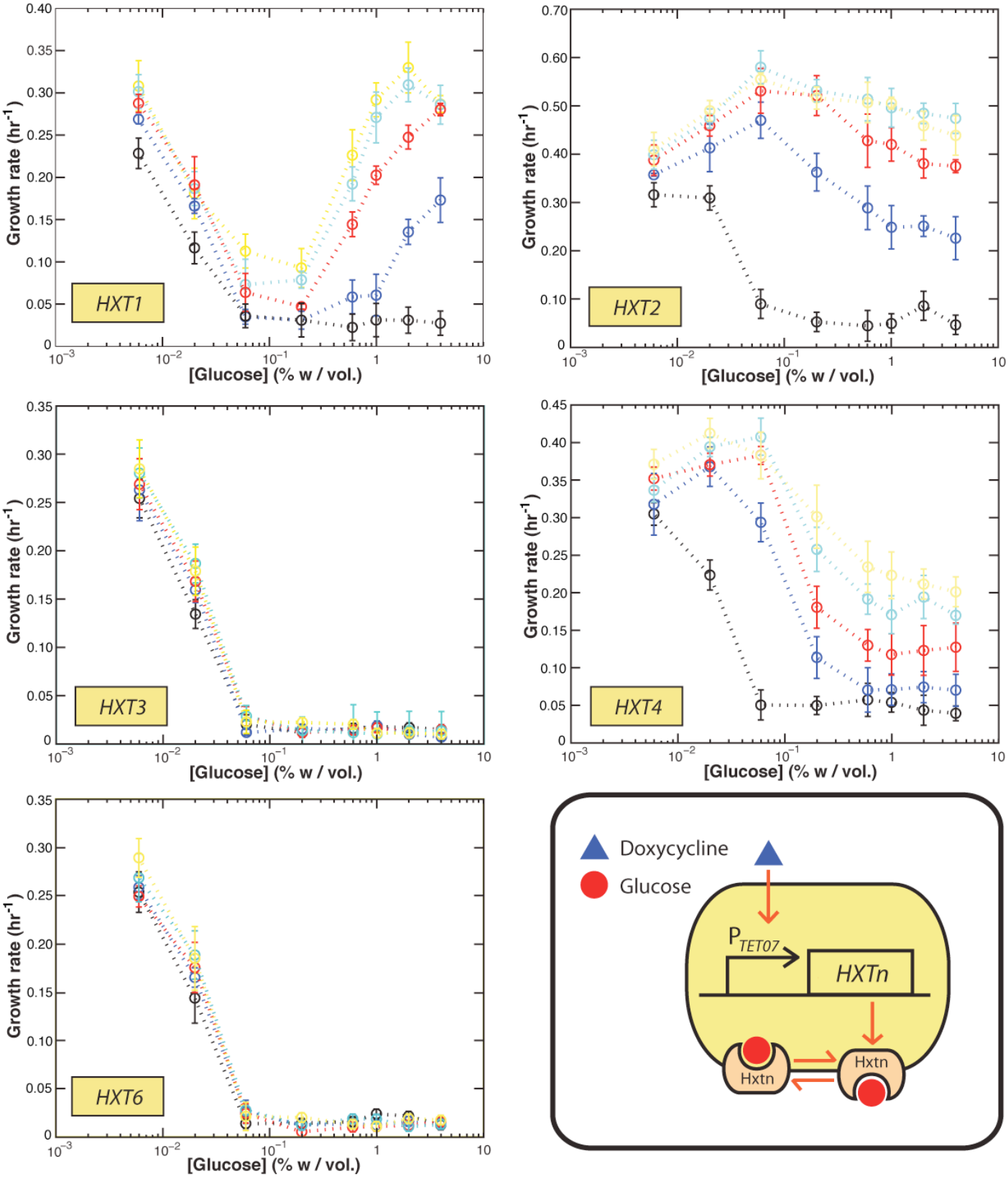

Supplementary Figure 3: (See next page for figure caption).

Supplementary Figure 3: Growth rate of single-*HXT* strains in various combinations of glucose and doxycycline concentrations. We measured the log-phase growth rate of the single-*HXT* strains in synthetic growth media containing doxycyline and glucose. These concentrations remained constant during each batch growth experiment. Each color corresponds to a particular value of doxycycline concentration as indicated in Supplementary Fig. 2. A curve of a given color shows how the growth rate changes as a function of the glucose concentration (at fixed doxycycline concentration). None of these strains' growth rates increase monotonically with an increase in the glucose level, unlike the parental wild-type strain (See Fig. 1). Depending on the initial glucose level, a further increase in the glucose level either increases or decreases the single-*HXT* strain's growth rate. Error bars, s.e.m.; n=3.

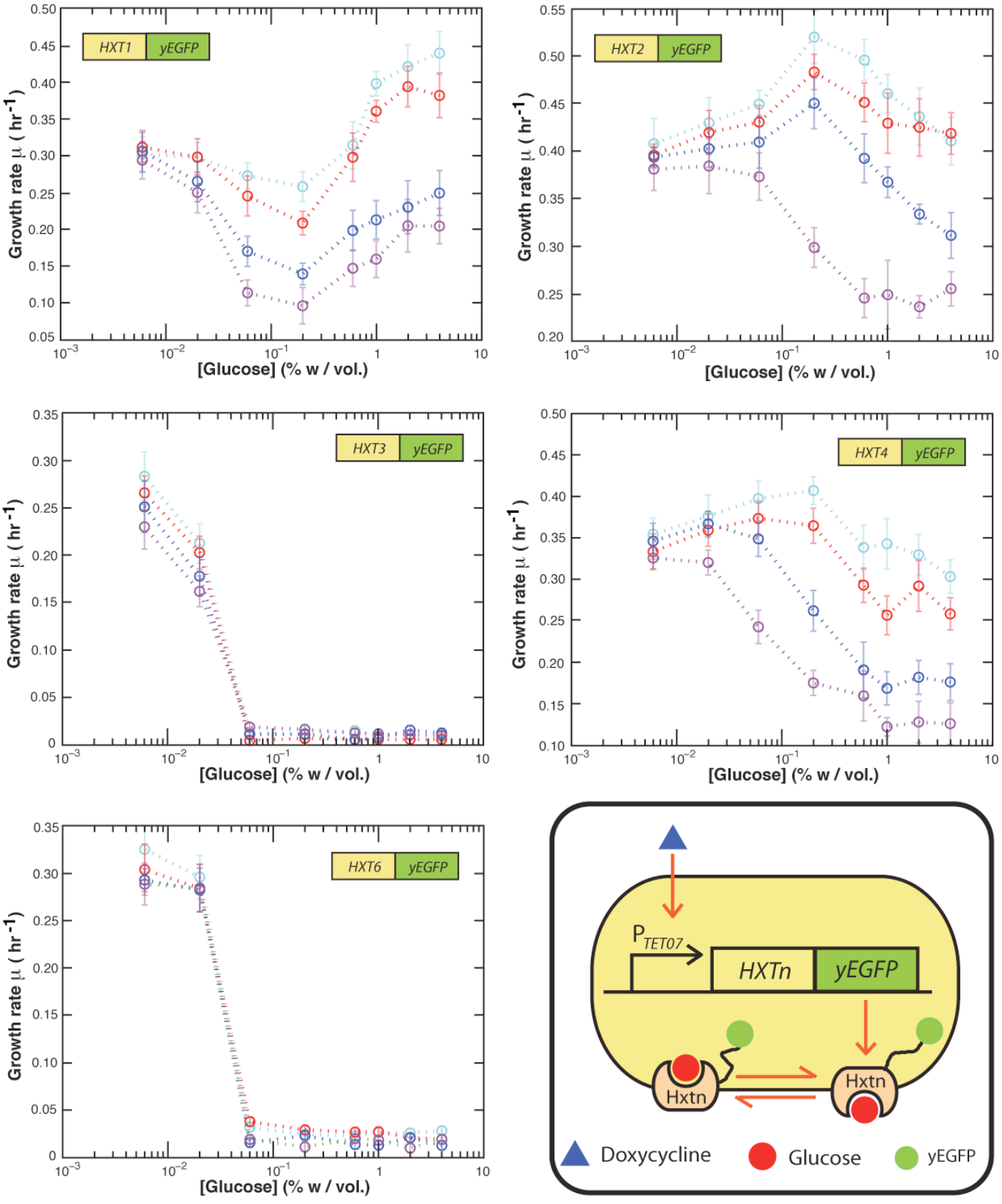

Supplementary Figure 4: (See next page for figure caption).

Supplementary Figure 4: Growth rate of fluorescent single-*HXT* strains (yEGFP fused to a *HXT* gene in each single-*HXT* strain) in various combinations of glucose and doxycycline concentrations. Each color corresponds to a particular value of doxycycline concentration as indicated in Supplementary Fig. 2 (purple represents [doxycycline] = 0.25 μg/ml). Fusing yEGFP to a *HXT* gene results in functional fluorescent single-*HXT* strains whose growth rates show the same key features that their non-fluorescent counterparts exhibit (Supplementary Fig. 3). These fluorescent strains thus exhibit the same apparent non-systematic behavior in their growth rates as their non-fluorescent counterparts. Error bars, s.e.m.; *n*=3.

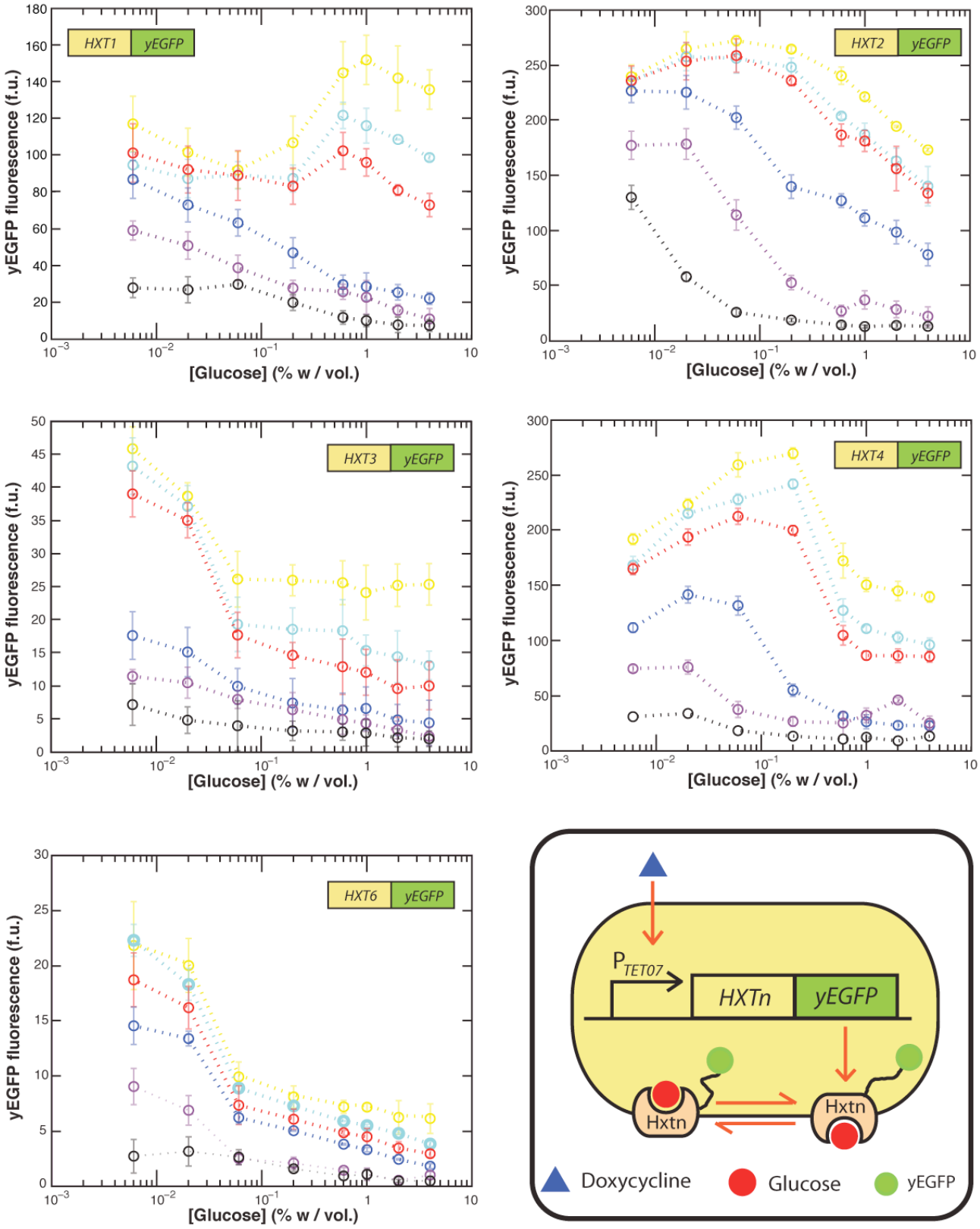

Supplementary Figure 5: (See next page for figure caption).

Supplementary Figure 5: Average, steady-state, single-cell yEGFP levels in the fluorescent single-*HXT* strains growing in various combinations of glucose and doxycycline concentrations. In the single-*HXT* strains with the yEGFP fused to the *HXT* gene, the relative number of Hxt proteins per cell was inferred from the average single-cell fluorescence measured using flow cytometer (See methods). Each color corresponds to a particular value of doxycycline concentration as indicated in Supplementary Fig. 2 (purple represents [doxycycline] = 0.25 μg/ml). The fact that single-cell fluorescence value changes as the glucose level changes (at constant doxycycline level), indicates an existence of post-transcriptional regulations of the Hxts. Indeed, previous works have revealed some glucose dependent post-transcriptional regulations of Hxts (e.g., endocytosis of Hxt6 & Hxt7 at high glucose levels)[4] and other metabolic genes[2,5]. We took into account the effect that such regulation has on glucose uptake by directly measuring the uptake rates. The cell's glucose uptake rate is determined by the combination of two parameters – the amount of Hxt protein in the cell and the extracellular glucose concentration. By measuring the glucose uptake rates, we found that all the single-*HXT* strains' glucose uptake rates monotonically increase when the glucose concentration increases (at fixed doxycycline level; Fig. 2 & Supplementary Fig. 7). This is because even though the number of Hxt protein in a cell may decrease when the glucose level rises (at fixed doxycycline level), this decrease is feeble: it is more than compensated by the accompanying increase in the glucose level, resulting in net increase in glucose uptake rate. This is confirmed by both our measured and calculated glucose uptake rates (Supplementary Figs. 6 & 7). Error bars, s.e.m.; *n*=3.

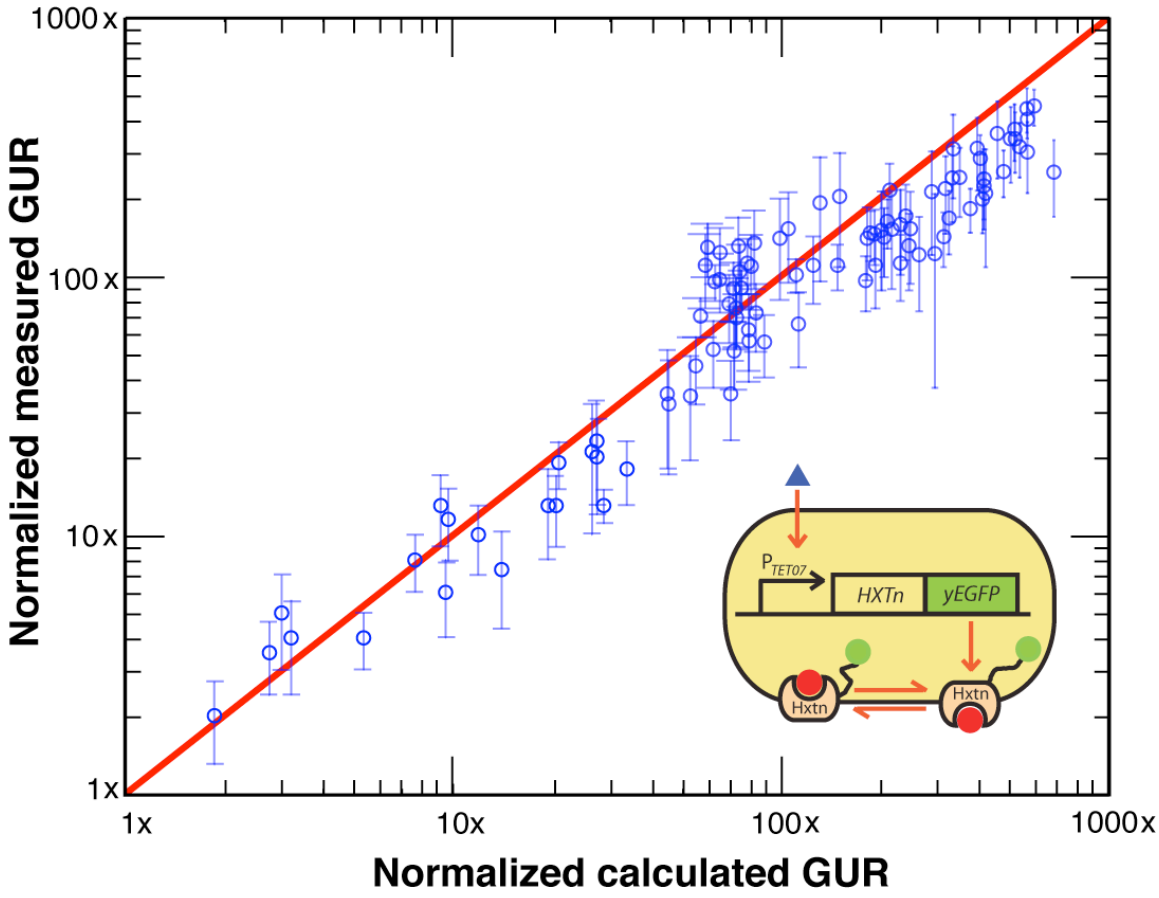

Supplementary Figure 6: Comparison of measured glucose uptake rate (GUR) with calculated GUR of the fluorescent single-*HXT* strains. The measured and calculated values of glucose uptake rate of all the fluorescent "single-*HXT*" strains are plotted together here. GURs are reported in normalized units to show that relative changes in both the measured and calculated GURs are in good agreement with each other. Error bars, s.e.m.; *n*=3.

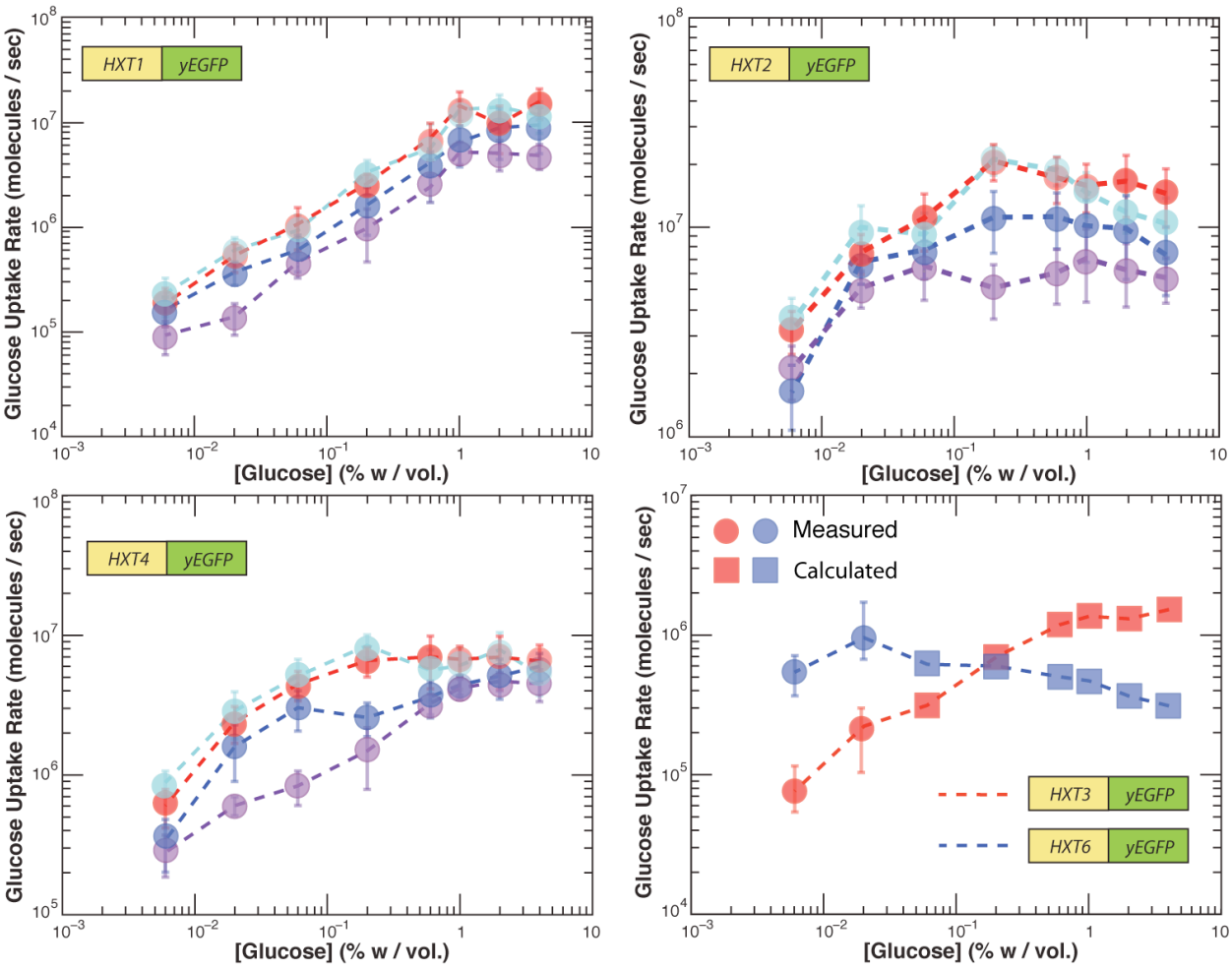

Supplementary Figure 7: Measured glucose uptake rates (GURs) of fluorescent single-*HXT* strains growing in various combinations of glucose and doxycycline concentrations. Each color corresponds to a particular doxycycline concentration as indicated in Supplementary Fig. 2 (purple represents [doxycycline] = 0.25 μg/ml). For "Hxt3-only" and "Hxt6-only" strains, only the GURs at [doxycycline] = 2.5 mg/ml are shown here for clarity. Since these two strains transiently approach near growth arrest for [glucose] > 0.02%, their GURs could not be measured using our method for [glucose] > 0.02%. Instead, we calculated their GURs as they transiently approached near growth arrest based on their yEGFP fluorescence (Supplementary Fig. 5). Close agreement between the measured and calculated GURs (Supplementary Fig. 6) gives us confidence in these calculated GURs. Error bars, s.e.m.; *n*=3.

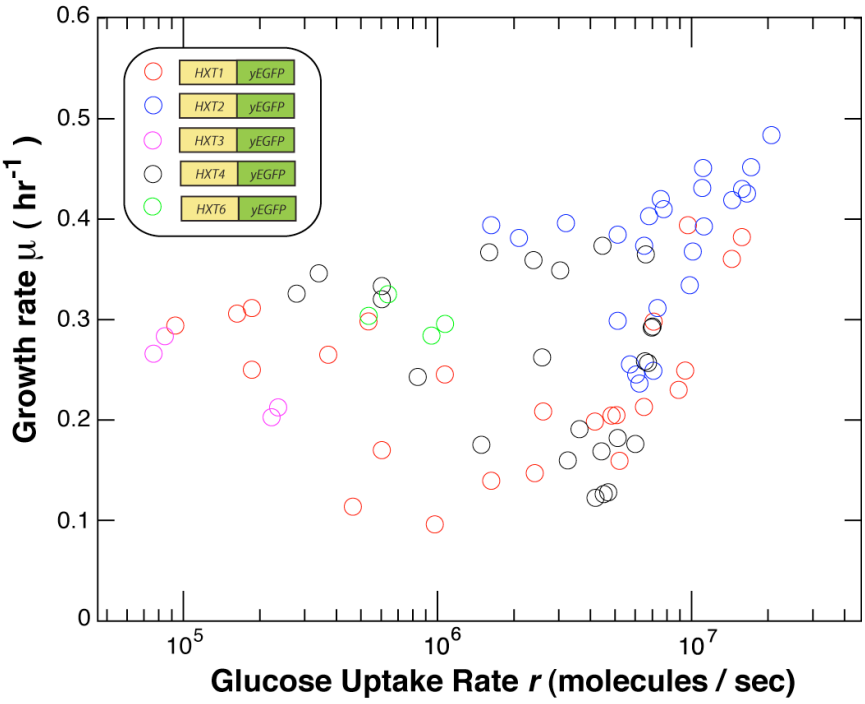

Supplementary Figure 8: Result of plotting the growth rate and the measured glucose uptake rate (GUR) of all the fluorescent single-*HXT* strains together. The color scheme represents the particular single-*HXT* strain to which the data points belong. The overlap of data points belonging to different single-*HXT* strains but at the same GUR and glucose concentration, along with the pattern emerged in Fig. 3b, together demonstrate that only the value of GUR but not which Hxt was responsible for the glucose import, is a factor in determining the growth rate. Coloring these data points by a single color results in Fig. 3a.

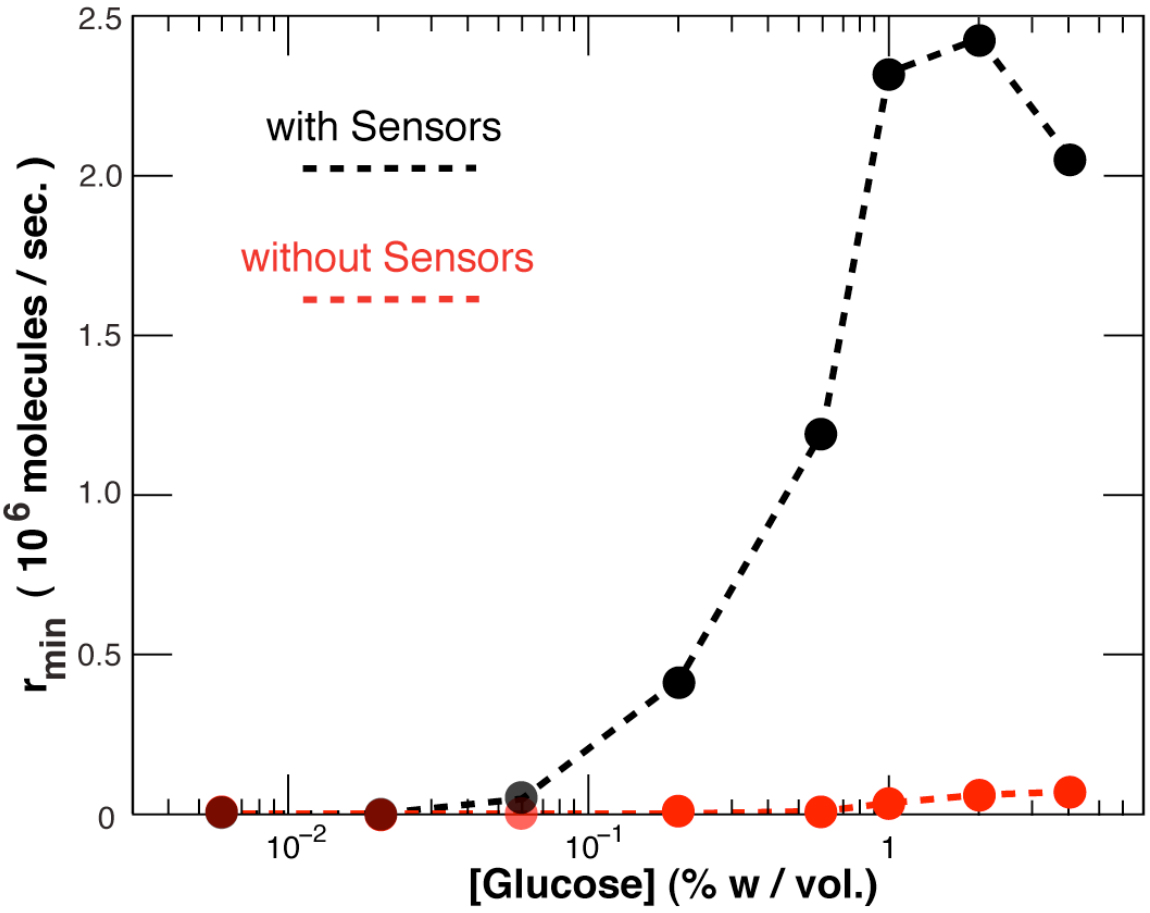

Supplementary Figure 9: Minimum glucose uptake rate r_{min} required for growth as a function of extracellular glucose *g*. $r_{\min} = r_c \exp\left(-\frac{\mu_c}{P(g)}\right)$ is the function describing these two curves, with *P(g)*, r_c, and μ_c fitted for a cell with the sensors (black line) and without the sensors (red line) (derived from Eqn [1] in main text; see Fig. 4d for "without sensor" strains). This shows that cells require a larger glucose uptake just to avoid growth arrest as more extracellular glucose is perceived.

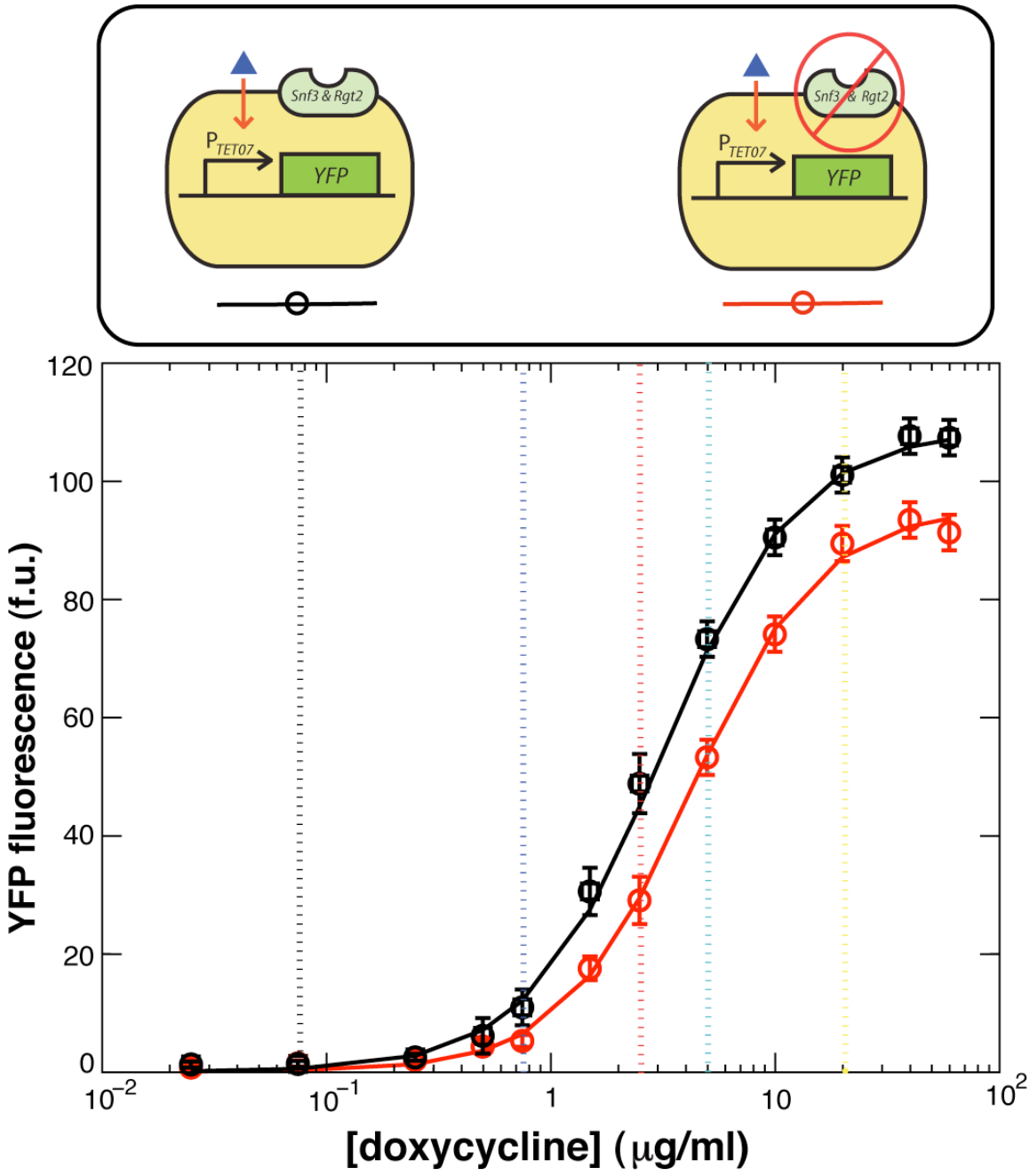

Supplementary Figure 10: Comparing the inducibility of P_{TET07} in HY4DCal5 (black line, with intact *SNF3* and *RGT2* genes) and in HY5FCal2 (red line, *snf3*Δ *rgt2*Δ). Single-cell fluorescence was measured using flow cytometer while HY4DCal5 and HY5FCal2 strains were in log-phase growth in standard synthetic media with 2% maltose and the indicated concentration of doxycycline. The colored vertical dashed lines indicate the concentrations of doxycyline used for characterizations of the "sensor-less" single-*HXT* strains (*snf3*Δ *rgt2*Δ) in subsequent supplementary figures. This plot shows that knocking out the two sensors makes only minor changes to the transcriptional activity of the promoter P_{TET07}. Error bars, s.e.m.; n=3.

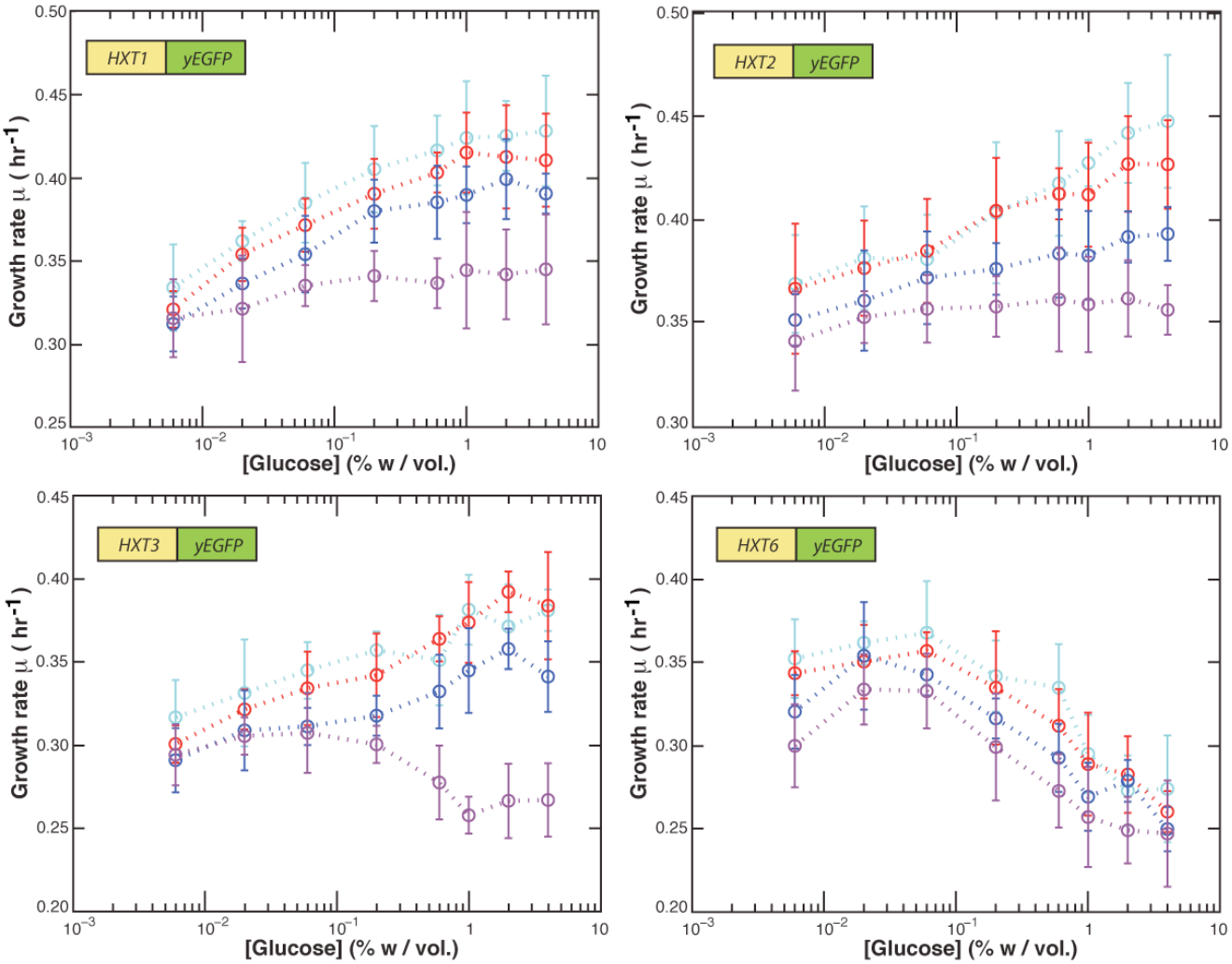

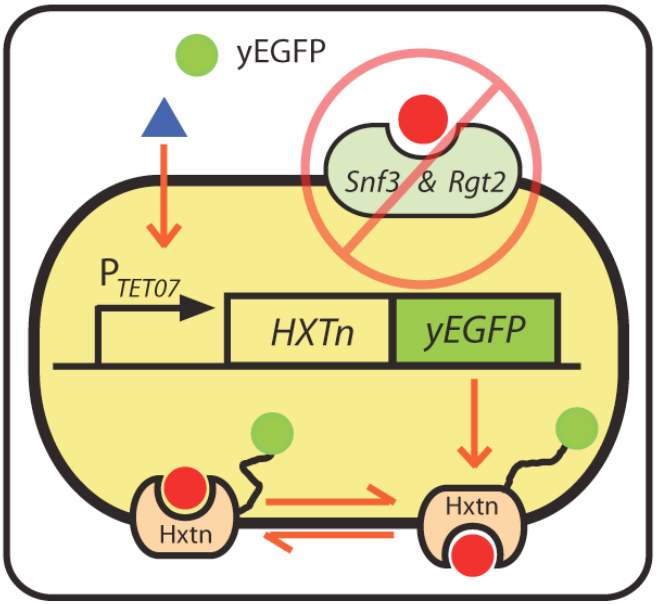

Supplementary Figure 11: Growth rates of fluorescent sensor-less single-*HXT* strains (*snf3*Δ *rgt2*Δ) in various combinations of glucose and doxycycline concentrations. Each color corresponds to a particular value of [doxycycline] indicated in Supplementary Fig. 10 (purple represents [doxycycline] = 0.25 μg/ml). These strains' growth rates behave in a starkly different manner from their sensor-intact counterparts (compare with Supplementary Fig. 4). "Hxt3-only" and "Hxt6-only" strains no longer approach near growth arrest when the two sensors are absent. Error, s.e.m. *n*=3.

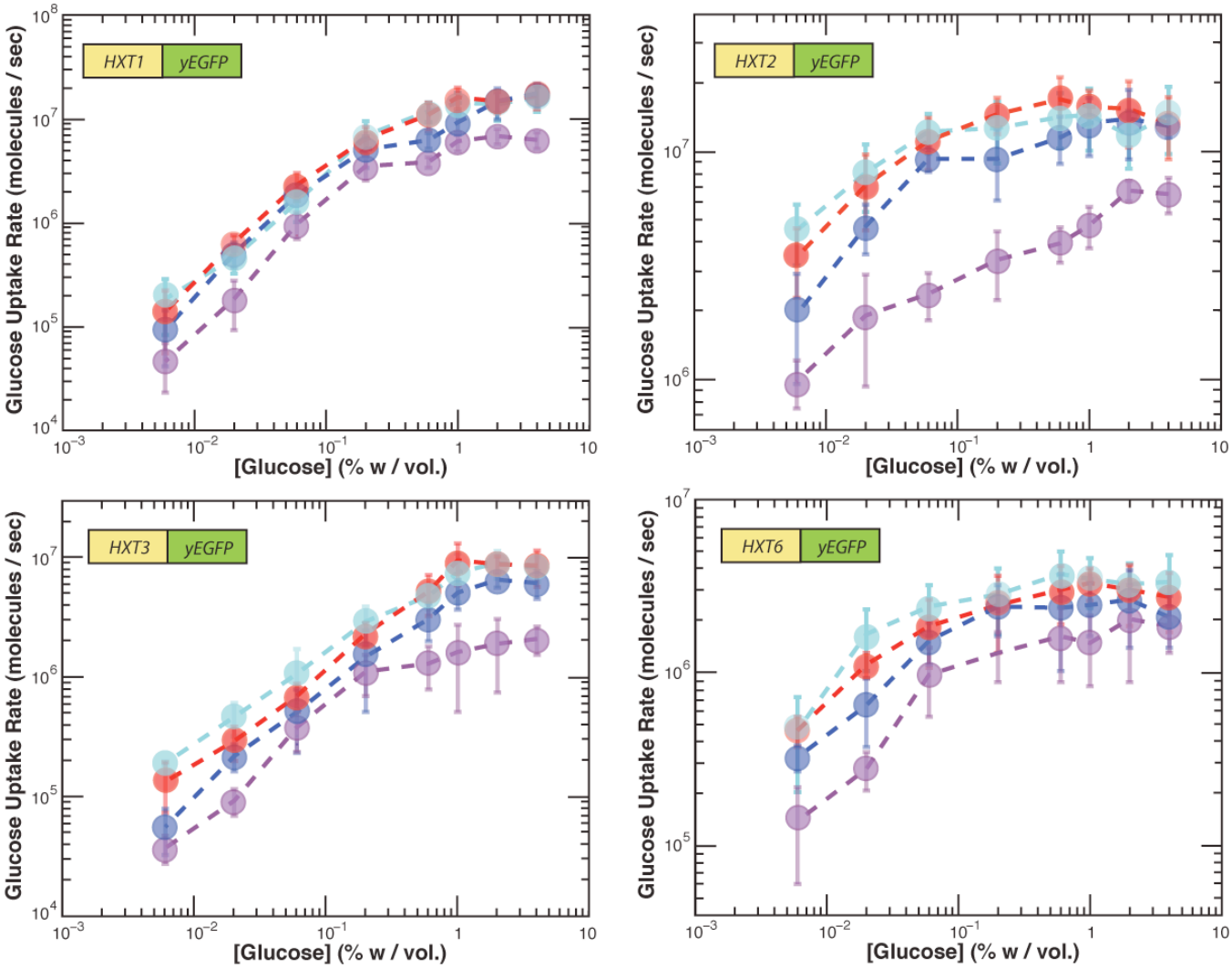

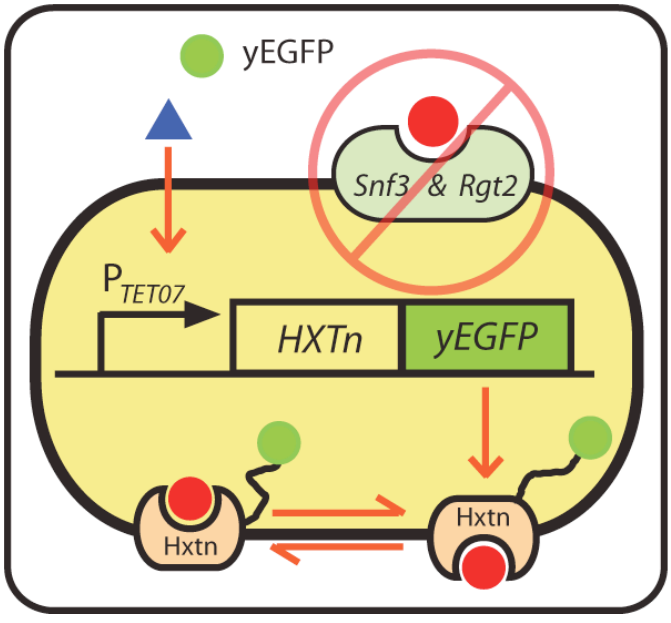

Supplementary Figure 12: Measured glucose uptake rates of sensor-less fluorescent single-*HXT* strains (*snf3*Δ *rgt2*Δ) in various combinations of glucose and doxycycline concentrations. Each color corresponds to a particular value of doxycycline concentration indicated in Supplementary Fig. 10 (purple represents [doxycycline] = 0.25 μg/ml). Knocking out the two glucose sensors hardly perturbs the glucose uptake rates of the single-*HXT* strains (compare with

Supplementary Fig. 7). However, the sensorless single-*HXT* strains' growth rates are qualitatively very different from those of their sensor-intact counterparts (can be seen by comparing Supplementary Fig. 11 with Supplementary Fig. 4). This is due to the diminished sensing ability of the sensorless strains, as indicated by the significant decrease in *P([glucose])* (Fig. 4c). Having the sensors knocked out impairs the cell's ability to perceive how much extracellular glucose is surrounding the cell. In particular, the cell acts as if there is less glucose than there actually is (decrease in *P([glucose])*). Error bars, s.e.m.; *n*=3.

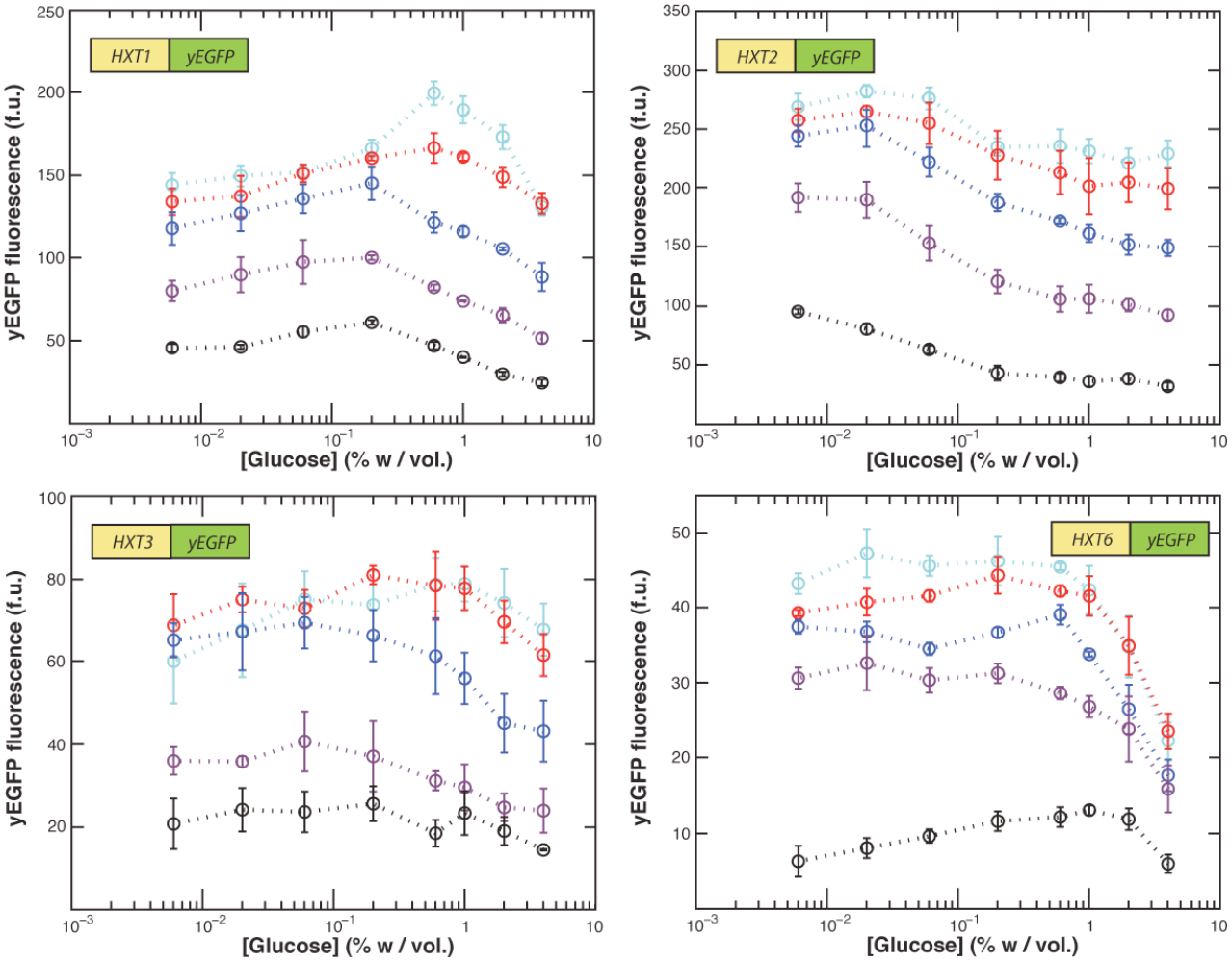

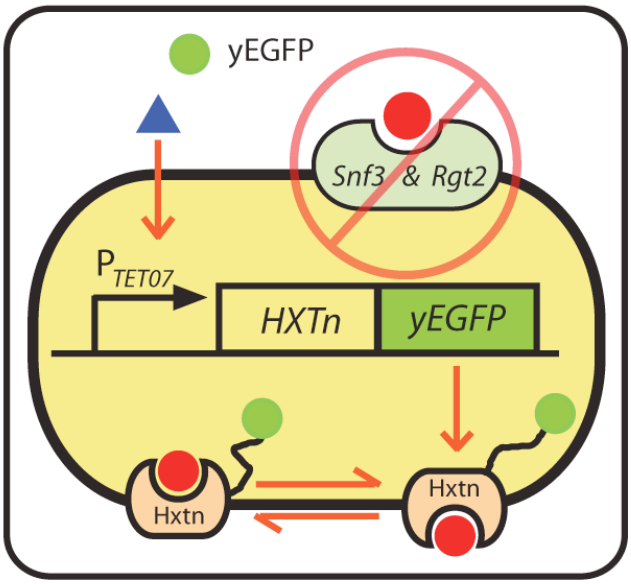

Supplementary Figure 13: Average single-cell, steady-state yEGFP fluorescence in the sensor-less single-*HXT* strains (*snf3*Δ, *rgt2*Δ) in various combinations of glucose and doxycycline concentrations. Each color corresponds to a particular value of doxycycline concentration indicated in Supplementary Fig. 10 (purple represents [doxycycline] = 0.25 μg/ml). The relative number of Hxt proteins per cell was inferred from the average single-cell fluorescence measured using flow cytometer (See methods). Post-transcriptional regulations of Hxts are observed in these "sensor-less" strains, just as we observed such regulations in the "single-*HXT*" strains with the sensors (See Supplementary Fig. 5). We took into account

the effect of these regulations on the glucose uptake by directly measuring the glucose uptake rates. As in the sensor-intact single-*HXT* strains (Supplementary Fig. 5), our measured glucose uptake rates of all the single-*HXT* strains monotonically increased as the glucose level increased (Supplementary Fig. 12). The reason for this is identical to the one given in the figure caption for Supplementary Fig. 5. Error bars, s.e.m.; *n*=3.

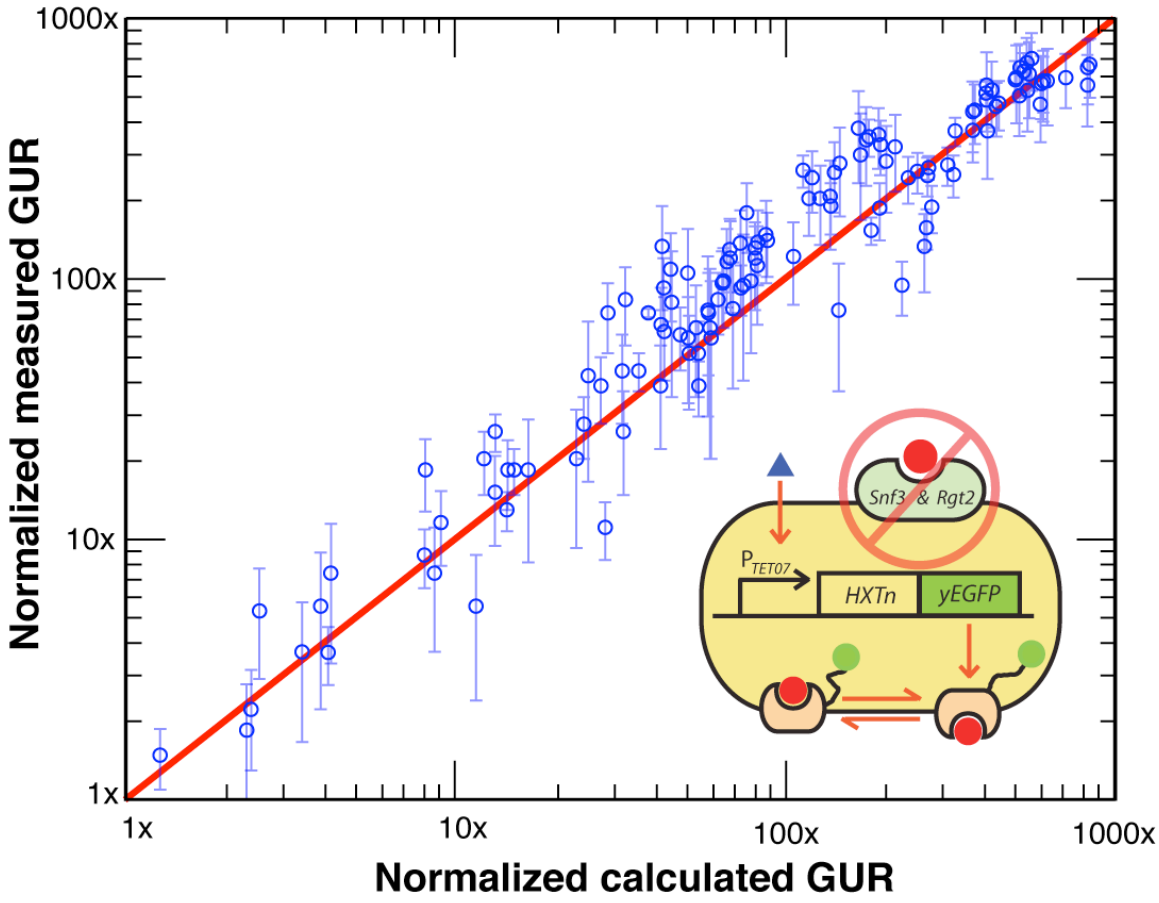

Supplementary Figure 14: Comparison of measured glucose uptake rate (GUR) and calculated GUR of the sensor-less fluorescent single-*HXT* strains (*snf3*Δ*rgt2*Δ). The measured and calculated values of glucose uptake rates of all the fluorescent single-*HXT* strains without the two glucose sensors (*snf3*Δ *rgt2*Δ) are compared here. GURs are reported in normalized units to show that the relative changes in both the measured and calculated GURs are in good agreement with each other. Error bars, s.e.m.; *n*=3.

a.

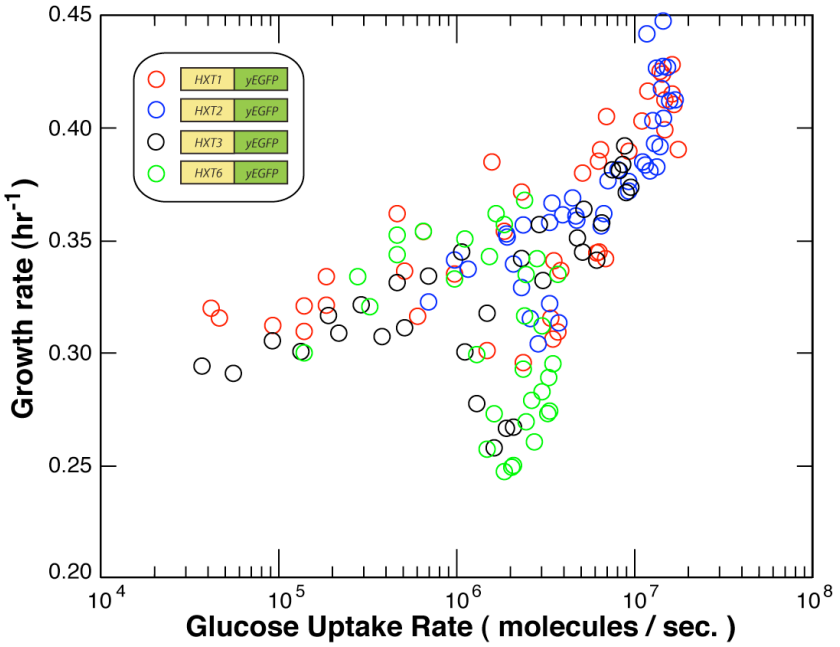

b.

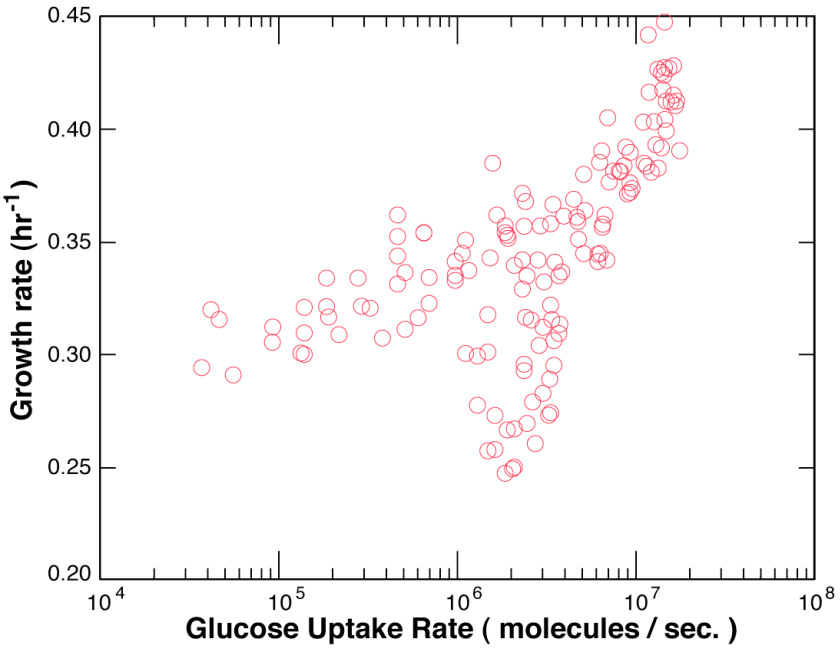

Supplementary Figure 15: Result of plotting the growth rate and the measured glucose uptake rate (GUR) of all the sensorless fluorescent single-*HXT* strains together. a. The color scheme represents the particular single-*HXT* strain (without *SNF3* and *RGT2*) to which the data points belong. The overlap of data points belonging to

different single-*HXT* strains but at the same GUR and glucose concentration, along with the pattern emerged in Fig. 4c, together demonstrate that only the value of GUR but not which Hxt was responsible for the glucose import, is a factor in determining the growth rate. **b.** Obtained by removing the colors from the data points shown in (a). This shows that for a particular value of glucose uptake rate, multiple growth rates are possible. This means that glucose uptake rate alone cannot specify the growth rate. But additionally coloring these data points according to the value of the extracellular glucose concentration leads to a striking pattern observed in Fig. 4c.

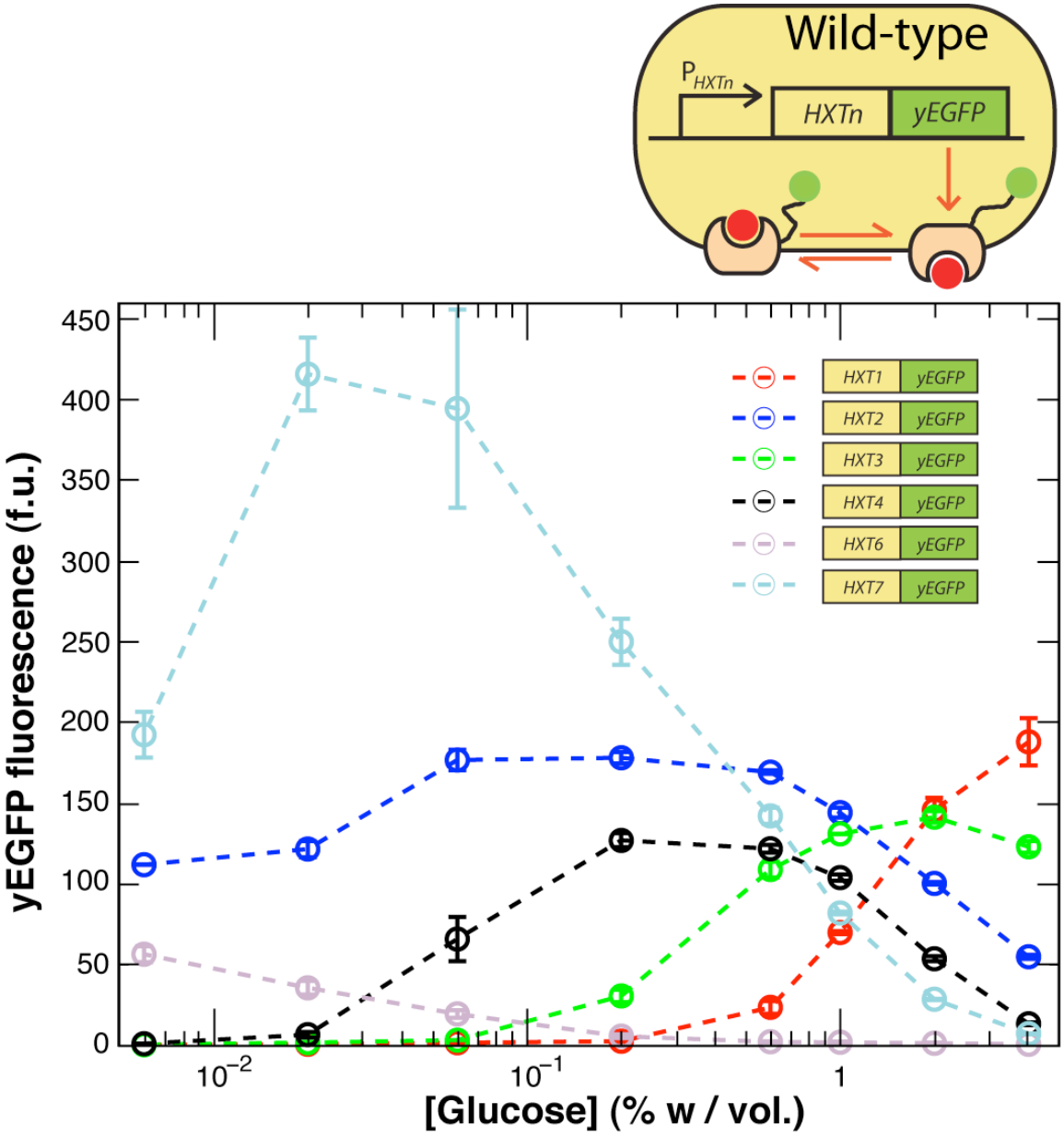

Supplementary Figure 16: Average single-cell fluorescence in the 'wild-type' strain (CEN.PK2-1C) with yEGFP fused to each *HXT* gene. The relative number of each Hxt protein present in the wild-type strain was inferred from these fluorescence levels. As in the single-*HXT* strains, the wild-type's glucose uptake rate that was calculated using these fluorescence values (See methods) was in close agreement with the directly measured glucose uptake rate (Supplementary Fig. 6 and Fig. 3b). Error bars, s.e.m.; *n*=3.

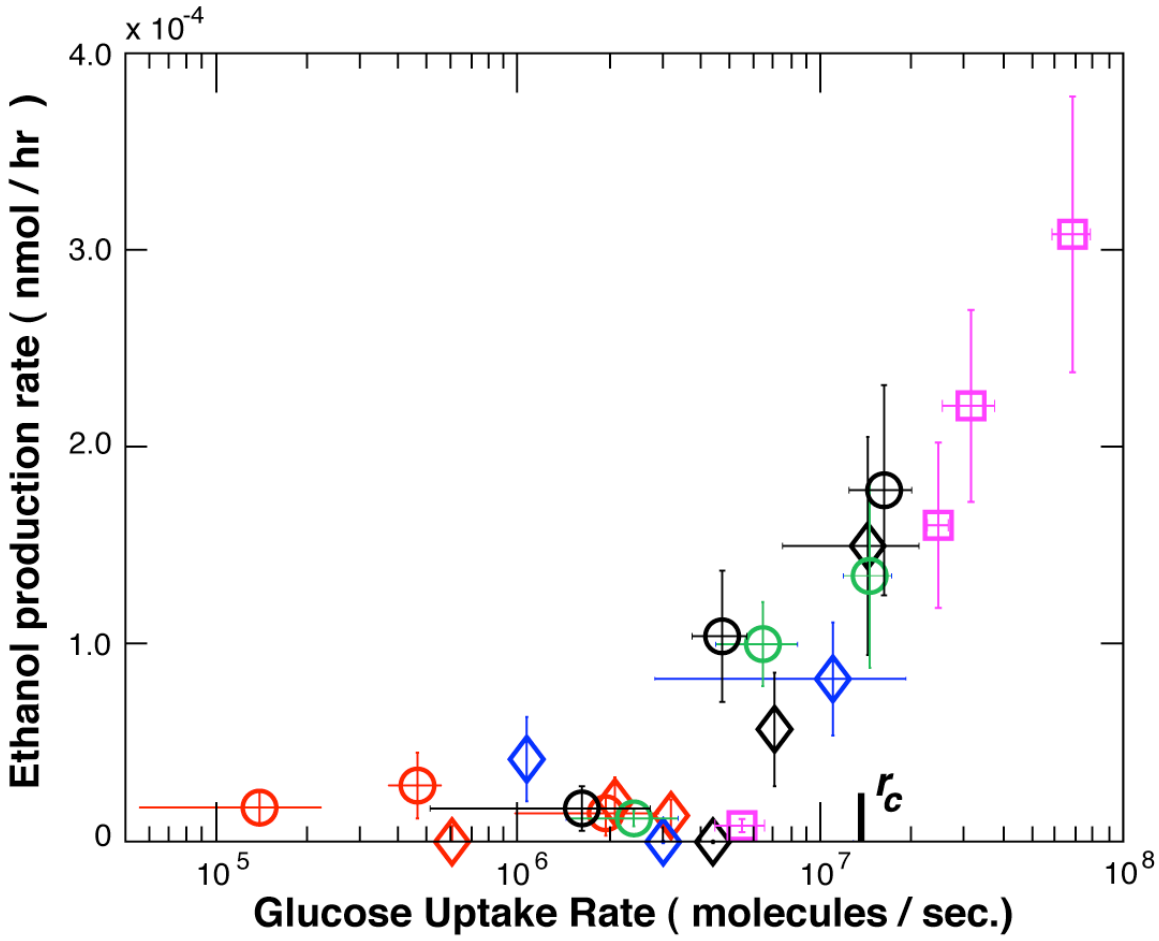

Supplementary Figure 17: Rate of ethanol production per cell suggests a shift from respiration to fermentation near the critical uptake rate r_c. Following a procedure essentially identical to the one used in measuring the glucose uptake rate (See methods), the average rate of ethanol production per cell was measured using a commerical ethanol assay kit (BioVision cat.#K620). Shown here are the ethanol production rates of the single-*HXT* strains with (diamonds) and without (circles) Snf3 and Rgt2 grown in various [glucose] (0.006% (red), 0.06% (blue), 0.2% (green), and 1% (black)). The ethanol production rates of the wild-type strain (squares) grown in these four values of [glucose] are also shown. The sharp increase in ethanol production rate indicates a shift from largely respirative to fermentative metabolism near the critical uptake rate r_c. Error bars, s.e.m.; n=3.

SUPPLEMENTARY REFERENCES

1. Yin, Z. *et al.* Glucose triggers different global responses in yeast, depending on the strength of the signal, and transiently stabilizes ribosomal protein mRNAs. *Molec. Microbiol.* **48**, 713-724 (2003).

2. Yin, Z., Hatton, L., & Brown, A.J.P. Differential post-transcriptional regulation of yeast mRNAs in response to high and low glucose concentrations. *Molec. Microbiol.* **35**, 553-565 (2000).

3. Ozcan, S. & Johnston, M. Three different regulatory mechanisms enable yeast hexose transporter (HXT) genes to be induced by different levels of glucose. *Mol. Cell. Biol.* **15**, 1564-1572 (1995).

4. Krampe, S., Stamm, O., Hollenberg, C.P., & Boles, E. Catabolite inactivation of the high-affinity hexose transporters Hxt6 and Hxt7 of *Saccharomyces cerevisiae* occurs in the vacuole after internalization by endocytosis. *FEBS Letters*, **441**, 343-347 (1998).

5. Bennet, M. R. *et al.* Metabolic gene regulation in a dynamically changing environment. *Nature* **454**, 1119-1122 (2008).

Strains used in this study:

Doxycycline Glucose yEGFP

"Single-*HXT*" strains

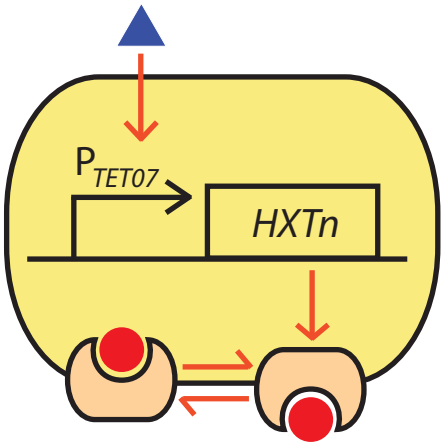

HY4D1 *LEU2* P_{TET07}: *HXTn*

	Strain name
HXT1	H1C3
HXT2	H2C1
HXT3	H3C1
HXT4	H4C9
HXT6	H6C4

"Single-*HXT*::yEGFP" strains

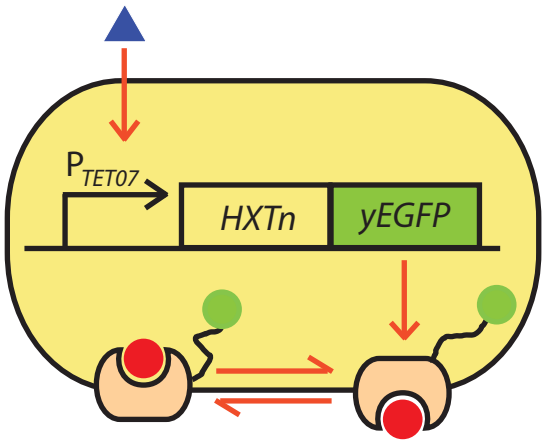

"Single-*HXT*" strain *Kan*^{R} *HXTn*::*yEGFP*

	Strain name
HXT1	H1C3Fus14
HXT2	H2C1Fus18
HXT3	H3C1Fus32
HXT4	H4C9Fus1
HXT6	H6C4Fus20

"Single-*HXT*" strains (Sensor-less)

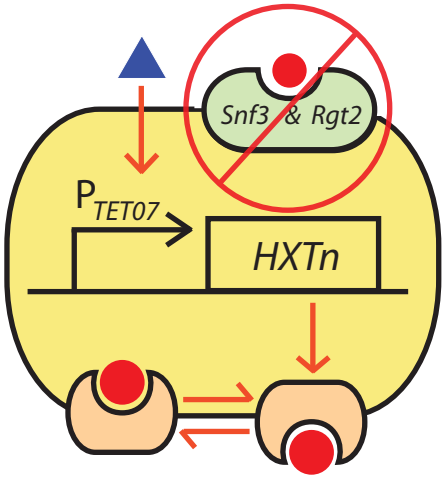

HY5F1 *LEU2* P_{TET07}: *HXTn*

	Strain name
HXT1	H1NS2
HXT2	H2NS5
HXT3	H3NS5
HXT4	H4NS2
HXT6	H6NS2

"Single-*HXT*::yEGFP" strains (Sensor-less)

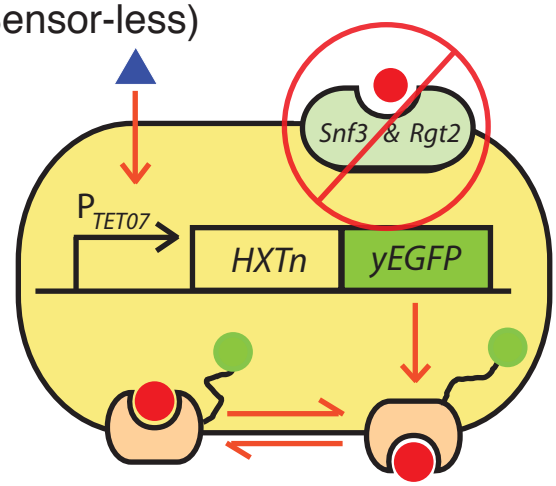

"Single-*HXT*" strain *Kan*^{R} *HXTn*::*yEGFP* (Sensor-less)

	Strain name
HXT1	H1NS2Fus30
HXT2	H2NS5Fus4
HXT3	H3NS5Fus2
HXT4	could not be made
HXT6	H6NS2Fus22

Strains used in this study (Continued):

Wild-type P_{HXTn}:*YFP*

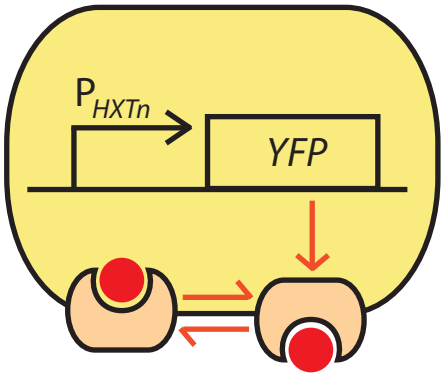

CEN.PK2-1C *LEU2* P_{HXTn} :*HXTn*

	Strain name
HXT1	H1S1
HXT2	H2S2
HXT3	H3S1
HXT4	H4S2
HXT7	H7S2

Wild-type *HXTn*::yEGFP

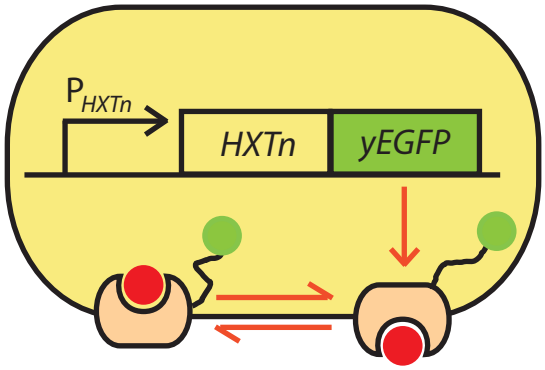

CEN.PK2-1C *Kan*^{R} *HXTn*::*yEGFP*

	Strain name
HXT1	CenH1Fus10
HXT2	CenH2Fus5
HXT3	CenH3Fus4
HXT4	CenH4Fus10
HXT6	CenH6Fus10
HXT7	CenH7Fus15

Strains for studying P_{TET07} induction:

Strain name		Genotype	Notes
HY4DCal5	EBY.VW4000	*HIS5 LEU2* P_{MYO2} *:rtTA* P_{TET07} *:YFP*	Used in Fig. S2.
HY5FCal2	EBY.VW5000	*HIS5 LEU2* P_{MYO2} *:rtTA* P_{TET07} *:YFP*	Used in Fig. S10.

Others:

Strain name	Genotype	Notes
HY4D1	EBY.VW4000 *HIS5* P_{MYO2}*:rtTA*	Common parent for all "single-*HXT*" strains (with sensors)
HY5F1	EBY.VW5000 *HIS5* P_{MYO2}*:rtTA*	Common parent for all "single-*HXT*" strains (*snf3*Δ *rgt2*Δ)
EBY.VW4000	(See Reference*)	*hxt1-17*Δ *RGT2* and *SNF3* intact. Gift from E. Boles.
EBY.VW5000	(See Reference*)	*hxt1-17*Δ *rgt2*Δ *snf3*Δ. Gift from E. Boles.
CEN.PK2-1C	(See Reference*)	"Wild-type" used in this study. Gift from E. Boles.

Note: EBY.VW4000 and EBY.VW5000 are both unable to grow on glucose since all HXTs as well as genes for transporters with minor glucose uptake capability had been deleted (hxt1-17Δ agt1Δ stl1Δ gal2Δ).

* R. Wieczorke, S. Krampe, T. Weierstall, K. Freidel, C. Hollenberg, and E. Boles. "Concurrent knock-out of at least 20 transporter genes is required to block uptake of hexoses in *Saccharomyces cerevisiae*", *FEBS Letters,* **464** (3), 123-128 (1999).